Title

A Bin and a Bulk Microphysics Scheme Can Be More Alike Than Two Bin Schemes

Journal

Journal of Advances in Modeling Earth Systems, 15(3)

ISSN

1942-2466

Authors

Hu, Arthur Z

Igel, Adele L

Publication Date

2023-03-01

DOI

10.1029/2022ms003303

JAMES | Journal of Advances in Modeling Earth Systems

RESEARCH ARTICLE
10.1029/2022MS003303

Key Points:

- Bulk and bin microphysics schemes with the same parameterizations simulate clouds more similarly than those simulated by two bin schemes
- Substantial differences between bin and bulk schemes are found only for collisions; they are reduced with a lower cloud-rain size boundary
- The advantages of using a bin scheme rather than a bulk scheme for microphysics may not be as large as previously thought

Correspondence to:
A. Z. Hu,
azqhu@ucdavis.edu

Citation:
Hu, A. Z., & Igel, A. L. (2023). A bin and a bulk microphysics scheme can be more alike than two bin schemes. *Journal of Advances in Modeling Earth Systems*, *15*, e2022MS003303. https://doi.org/10.1029/2022MS003303

Received 14 JUL 2022
Accepted 17 FEB 2023

Author Contributions:
Conceptualization: Adele L. Igel
Data curation: Arthur Z. Hu
Formal analysis: Arthur Z. Hu, Adele L. Igel
Funding acquisition: Adele L. Igel
Investigation: Arthur Z. Hu
Methodology: Arthur Z. Hu, Adele L. Igel
Project Administration: Adele L. Igel
Software: Arthur Z. Hu, Adele L. Igel
Supervision: Adele L. Igel
Validation: Arthur Z. Hu, Adele L. Igel
Visualization: Arthur Z. Hu
Writing – original draft: Arthur Z. Hu
Writing – review & editing: Arthur Z. Hu, Adele L. Igel

A Bin and a Bulk Microphysics Scheme Can Be More Alike Than Two Bin Schemes

Arthur Z. Hu[1] **and Adele L. Igel**[1,2]

[1]Atmospheric Science Graduate Group, University of California Davis, Davis, CA, USA, [2]Department of Land, Air and Water Resources, University of California Davis, Davis, CA, USA

Abstract Bin and bulk schemes are the two primary methods to parameterize cloud microphysical processes. This study attempts to reveal how their structural differences (size-resolved vs. moment-resolved) manifest in terms of cloud and precipitation properties. We use a bulk scheme, the Arbitrary Moment Predictor (AMP), which uses process parameterizations identical to those in a bin scheme but predicts only moments of the size distribution like a bulk scheme. As such, differences between simulations using AMP's bin scheme and simulations using AMP itself must come from their structural differences. In one-dimensional kinematic simulations, the overall difference between AMP (bulk) and bin schemes is found to be small. Full-microphysics AMP and bin simulations have similar mean liquid water path (mean percent difference <4%), but AMP simulates significantly lower mean precipitation rate (−35%) than the bin scheme due to slower precipitation onset. Individual processes are also tested. Condensation is represented almost perfectly with AMP, and only small AMP-bin differences emerge due to nucleation, evaporation, and sedimentation. Collision-coalescence is the single biggest reason for AMP-bin divergence. Closer inspection shows that this divergence is primarily a result of autoconversion and not of accretion. In full microphysics simulations, lowering the diameter threshold separating cloud and rain category in AMP from 80 to 50 μm reduces the largest AMP-bin difference to ∼10%, making the effect of structural differences between AMP (and perhaps triple-moment bulk schemes generally) and bin even smaller than the parameterization differences between the two bin schemes.

Plain Language Summary There are two primary ways to predict how clouds form and evolve. In a model grid box, bulk schemes typically predict the evolution of just the total number and mass of cloud droplets, whereas bin schemes not only keep track of total amount but also the number of droplets of different sizes. Bulk schemes are more computationally efficient than bin schemes, but bin schemes are usually assumed to be more accurate. This study aims to reveal how such differences affect their prediction of clouds. Our results show that small droplets colliding and combining to form raindrops is the only process that leads to large differences between bin and bulk schemes. Other individual processes, including droplet activation, condensation, evaporation, and sedimentation, contribute substantially less to differences between the two schemes. These results suggest that the advantages of using a bin scheme may not be as large as previously thought.

1. Introduction

Modeling clouds is hard. As noted in great detail in Morrison, van Lier-Walqui, Fridlind, et al. (2020), the two biggest obstacles are (a) the sheer number of cloud and precipitation particles to predict and (b) the lack of the fundamental understanding of microphysical processes involved. With quintillions of droplets in a typical cloud, it is infeasible to predict the evolution of each droplet and its environment. In addition, there does not exist a fundamental governing equation or benchmark model that can help inform the modeling of microphysics in larger scale, unlike other subgrid physical processes such as radiation, turbulence, and convection. Clouds are thus only modeled from a macroscopic perspective with its parameterizations determined empirically. Aside from the more recently developed Lagrangian superdroplet method (e.g., Shima et al., 2009), the two most well-established microphysics scheme types are the bulk microphysics scheme and the bin microphysics scheme. Bin schemes keep track of the number of droplets of within discrete size or mass ranges (i.e., size-resolved or mass-resolved), allowing the particle size distribution (PSD) to evolve freely but is therefore computationally expensive (A. P. Khain et al., 2015). On the other hand, bulk schemes predict quantities proportional to moments of the PSD (i.e., moment-resolved), typically mass and number concentration (e.g., Kessler, 1969; Lin

et al., 1983; Meyers et al., 1997). Albeit not a required feature for bulk schemes in principle, they also typically have a separate liquid water category (cloud mode and rain mode) and prescribe a gamma probability distribution function (PDF) for the PSD, which is less flexible than bin schemes but computationally efficient enough to model large-scale weather systems and global climate. This difference in PSD treatment between the two is known as their structural difference. In practice, however, they are also different on another level—how physical processes and properties are parameterized (A. P. Khain et al., 2015). This includes terminal velocity-diameter relationships, mass-diameter relationships, the collision-coalescence parameterization, the droplet activation parameterization, the condensation formulation, etc. Since the parameterizations are not easily convertible from one scheme to another, separating the importance of these two types of difference has been difficult. In this study, we aim to isolate the structural difference from the parameterization difference between bin and bulk schemes.

Although there has been a great number of studies that compared bin and bulk schemes, their objectives are mainly to assess the advantages and disadvantages of *existing* schemes (Fan et al., 2012, 2016; Li et al., 2009; Seifert & Beheng, 2006a, 2006b). In these studies, the explanation for the difference between simulations performed by bin and bulk schemes are almost never related to their structural difference. Instead, it was pointed out that the possible reasons could be (a) the lack of inclusion of an aerosol budget, (b) wide adoption of saturation adjustment, and (c) parameterization of autoconversion that was derived under a narrow range of conditions (Fan et al., 2016). Despite being valuable addition to our knowledge of the existing models, none of these studies mentioned the relative importance of a model's structure and parameterization choices on the final prediction. However, it is well known that microphysics parameterization choices can have a large impact on simulations. For example, in an idealized supercell simulation, Falk et al. (2019) found that the terminal speed parameterization is a greater factor in determining how a supercell splits than the choice of a bin versus bulk microphysics scheme. Another study by Johnson et al. (2015) showed that the accumulated precipitation from a deep convective cloud can vary from 0 to 70 mm just by adjusting 11 cloud and aerosol parameters within physically reasonable ranges within a single bulk scheme. Parameterization sensitivity is not limited to bulk schemes, especially when ice microphysics is involved. This is because, unlike liquid hydrometeors, ice particles are observed with a variety of shapes and habits in the atmosphere, which poses challenges on predicting how they fall and interact with other ice or liquid particles (Morrison, van Lier-Walqui, Fridlind, et al., 2020). The case study of a squall line event discussed in Xue et al. (2017) revealed that different bin schemes can behave quite differently regarding reflectivity patterns, cold pool extent, and thermodynamic structure, although many of the differences can be attributed to the ice-phase parameterization. Nevertheless, they showed that the spread among the bin schemes was qualitatively similar to the spread among the bulk schemes tested in Morrison et al. (2015), further hinting that model intercomparisons between bin and bulk schemes should be done carefully. These findings, again, prompt the question, how similar would bulk and bin schemes be if they were only different structurally?

It is a valuable question to ask for two reasons: (a) because knowing how bin and bulk schemes are different structurally can help us understand both the limitation and the true capability of a moment-resolved scheme and (b) it may also give us confidence in the future development of bulk schemes if the bin-bulk differences are found to be small. Additionally, the efficiency of bulk schemes is still required for large scale simulations in the foreseeable future despite the exponential increase in computational power and as such continued improvement of bulk schemes is necessary.

Many efforts have been made toward narrowing down the effect of different microphysics schemes by prescribing a velocity field and disallowing feedbacks from the microphysics. Morrison and Grabowski (2007) compared their two-moment (2M) bulk scheme with a bin model as a benchmark in this way. They found that the simulations performed by bulk and bin schemes were similar for mean effective radius and cloud water path with the bulk simulations having a slightly larger mean effective radius. They also noted that the uncertainty was most likely a result of their relative dispersion diagnostic equation. Shipway and Hill (2012) conducted a similar study. They concluded that the 2M bulk schemes generally perform more similar to a bin scheme than 1M bulk schemes do but produce larger precipitation peaks than any other schemes, which is a result of their excessive size sorting problem. Excessive size sorting is a result of the structure of bulk schemes (Morrison, 2012) and exists in most 2M schemes and can be improved considerably with a three-moment (3M) bulk scheme (J. A. Milbrandt & McTaggart-Cowan, 2010; Jason A. Milbrandt & Yau, 2005; Shipway & Hill, 2012).

Even with the same prescribed dynamics, the different predictions that the microphysics routines in bulk and bin schemes make can still be a combined effect of structure and parameterization. To address this problem, Igel (2019) (hereafter I19) designed the Arbitrary Moment Predictor (AMP) to isolate and compare the effect of structural

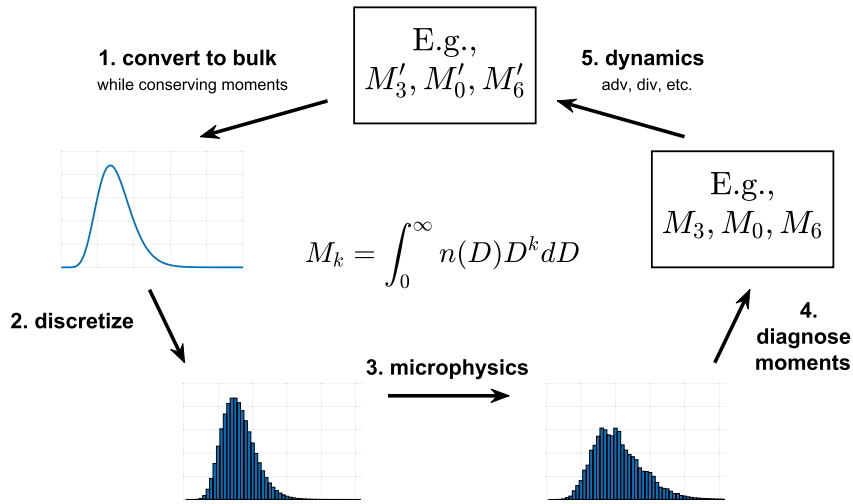

Figure 1. The steps taken by AMP to predict the moments of one hydrometeor species. The equation at the center is the definition of *k*th moment. The microphysics processes in Step 3 can include any combination of condensation, evaporation, collision-coalescence, and/or sedimentation. M_k' after Step 5 is the *k*th moment M_k after dynamics is calculated. Note that Step 5 (dynamics) is performed by the dynamical core and is not part of AMP.

difference alone. At its core, AMP is a bulk scheme that assumes a gamma PSD and predicts moments, but it uses a bin scheme to do microphysics calculations. The scheme was designed not necessarily to replace existing bulk schemes, but to study the effect of the structural differences between bulk and bin schemes. All differences between simulations with AMP and simulations with its underlying bin scheme can be attributed to structural differences. Igel (2019) performed simulations in an idealized box model with individual processes turned on (condensation, evaporation, and collision-coalescence). In the idealized box model, it was found that AMP could mimic its bin counterpart for condensation and evaporation quite closely, whereas AMP and its underlying bin scheme could produce substantially different evolutions of rain water production during collision-coalescence. Igel et al. (2022) (hereafter I22) further explored the reasons for poor performance of AMP during collision-coalescence.

Following on from I19 and I22, this study increases the complexity from single-process box model simulations to 1D kinematic simulations with all warm phase microphysical processes turned on. The objective of this study is to examine processes not previously discussed in I19 and I22 (droplet activation, sedimentation) and to examine how the interactions between all microphysical processes forced by simplified dynamics magnify (or not) the different performances of bin and bulk schemes due to their structural differences. Although 2M bulk schemes are still the default and AMP can be configured to be either 2M or 3M, simulations tested in this paper will only the 3M AMP because unlike a 2M bulk scheme, a 3M bulk scheme can prognostically evolve the width of the PSD. In this study, we configure AMP to act like a typical 3M bulk scheme in which the 3rd, 0th, and 6th moments of the cloud and rain size distributions are predicted. This moment combination was found to be among the best for 3M schemes for individual processes like condensation, evaporation, collision-coalescence (I19), and sedimentation (J. A. Milbrandt & McTaggart-Cowan, 2010).

The rest of the paper is organized as follows. Section 2 briefly explains the mechanics of AMP. Section 3 describes the model setup, the simulations with different combinations of microphysical processes, and the range of initial conditions used for these simulations. Section 4 presents the results from the simulations. Section 5 gives the concluding remarks of the findings.

2. Mechanics of AMP: Bin Physics Put Into a Bulk Scheme

In order to isolate the structural difference from the parameterization difference between bin and bulk schemes, a hybrid bin-bulk microphysics scheme, AMP, was designed (I19). Figure 1 is a conceptual schematic of the procedures of AMP:

1. At the beginning of each time step, parameters of a gamma distribution are diagnosed from the moment values (M_k') of a PSD from the last time step.
2. The gamma-shaped size distribution is then discretized.

3. The discretized PSD is passed into bin microphysics scheme routines, which include any combination of condensation, evaporation, collision-coalescence, and/or sedimentation.
4. Moment values (e.g., 3rd, 0th, and 6th) are diagnosed after the microphysics routines complete.
5. These moment values (M_k) are passed into the dynamics routines (advection, divergence, etc.), which is performed by the dynamical core and is not part of AMP. The products are the predicted moment values ($M_k{}'$) for the next time step.

AMP treats each hydrometeor category separately. In this study, we have two hydrometeor categories: cloud and rain, with a diameter threshold of ~80 μm, as adopted by many existing bulk microphysics scheme (Beheng, 1994; Berry & Reinhardt, 1974; Lee & Baik, 2017; Seifert & Beheng, 2001; Wang et al., 2013), although an alternative threshold of 50 μm will be examined in Section 4.4. If there is mass in both categories, their discretized PSDs are concatenated before being passed into the microphysics routine (Step 3).

Since no single bin scheme is perfect, we implemented two underlying bin schemes into AMP: the Hebrew University spectral bin microphysics (SBM; A. Khain et al., 2004) and the Tel Aviv University (TAU) bin scheme (G. Feingold et al., 1988; Tzivion et al., 1987, 1999). The inclusion of the TAU scheme as an option is new to AMP in this study. The most prominent difference between these two bin schemes is that HU-SBM only predicts the mass for each droplet size bin, whereas TAU predicts both mass and number. The inclusion of two bin schemes allows us to assess the relative importance of the AMP-bin difference compared to the difference between two bin scheme types. All simulation cases in this study are thus performed with four microphysics schemes, which we denote as AMP-SBM, bin-SBM, AMP-TAU, and bin-TAU.

Note that we do not include an aerosol scheme in any test. Rather we specify an aerosol concentration that is a constant and droplet activation is parameterized by calculating the local cloud condensation nuclei (CCN) concentration and comparing it with the local droplet concentration. If the CCN concentration exceeds the droplet concentration, new droplets are formed. The calculation of the CCN concentration is different in the two bin schemes. More information about the representation of this process and all other processes may be found in the references above.

In summary, AMP is structurally a bulk scheme with bin scheme parameterizations. As such, comparing simulations with AMP with its underlying bin scheme sheds light on the structural differences between bulk and bin schemes. With the ability to switch each microphysical and dynamical process on and off, we can pinpoint the specific process in the model that leads to the differences in the simulation results by AMP and bin schemes, which will give us insights into the fundamental limitations of moment-resolved schemes with prescribed functional forms. A more detailed description of AMP can be found in Section 2 and Appendix A of I19.

3. Model Setup: 1D Simulations

This study builds on the box model AMP simulations performed by I19 and I22 by incorporating advection into the testing and extending the simulation into a 1D environment by utilizing the Kinematic Driver (KiD; Shipway & Hill, 2012). The key feature of KiD is that it prescribes a kinematic framework without the feedback from the microphysical processes (latent heat release, condensate loading, etc.). Despite being idealized, the benefit of this feature is that it simplifies the interpretation of the results so that any differences between model outputs from two different microphysics schemes must come directly from the schemes themselves rather than from complex feedbacks between microphysics, thermodynamics, and dynamics. This is therefore a natural continuation of the box model in the previous work while retaining a large degree of simplicity. As noted in the previous section, although AMP can be configured to conserve any combination of two or three moments, all simulations in this study resemble a typical 3-moment bulk scheme, that is, predicting the conventional 3rd, 0th, 6th moments.

In this study, 1D (column) "full microphysics" simulations are designed to mimic shallow warm cumulus clouds. By "full microphysics" we mean that droplet activation, condensation, evaporation, sedimentation, and collision-coalescence are all active. In these full microphysics tests, the initial conditions are based on KiD test case #102 (see the KiD documentation) which specifies an oscillating vertical velocity field along with initial temperature and relative humidity. Figure 2 shows the prescribed vertical velocity and the initial relative humidity profile. Note that the wind field is only set to advect vapor and hydrometeors and the temperature field is held constant in time. To cover a wide range of aerosol and dynamic conditions, we run a suite of simulations with vertically constant aerosol concentration (N_a) that cover aerosol environments from maritime (100/cc)

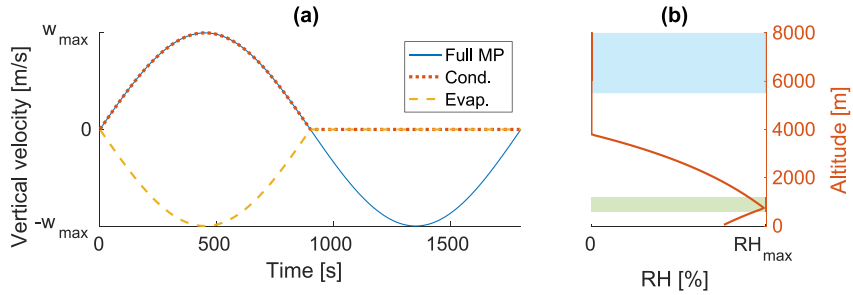

Figure 2. (a) Prescribed vertical velocity of the field for full microphysics, cases with condensation (updraft only), and cases with evaporation (downdraft only). (b) Initial relative humidity (RH) profile. The default $RH_{\max} = 100\%$ unless otherwise specified in Figure 3. The light green band represents the height and thickness of the initial layer of water for collision-coalescence and evaporation cases, and the light blue one represents that for the sedimentation case.

to continental (1600/cc) and dynamics from calm ($w_{\max} = 1\,\mathrm{m/s}$) to vigorous ($w_{\max} = 16\,\mathrm{m/s}$). As mentioned earlier, two pairs of microphysics schemes (AMP-SBM and bin-SBM, AMP-TAU and bin-TAU) are tested for each case to increase the robustness of the results.

We also run a systematic series of tests in which one or more microphysical processes is turned off in order to ascertain the contribution of individual processes to the total difference between the AMP and bin schemes. Figure 3 summarizes the simulations in this study: four sets of simulations with only a single process turned on, each with its respective initial condition suite (bottom row), along with three sets of simulations with combined processes and the same initial conditions as described above (left edge).

In all cases with condensation and droplet activation turned on (cases a, b, c, d), simulations are initialized with the same conditions as the full microphysics simulations. In cases b-d, evaporation is eliminated by holding the vertical wind speed at 0 m/s after the first half of the velocity oscillation (Figure 2a, orange dotted line).

In the cases without condensation or droplet activation (case e, f, g), we are required to initialize the simulation with existing condensed water. For the collision-coalescence case (e), water is initialized between 600 and 1200 m with sizes in the cloud droplet category (initial mean mass diameter $\overline{D}_m = 15 - 27\,\mu\mathrm{m}$) and with the shape parameter ranging from 1 to 9. No vertical wind is included and so these simulations are essentially the same as box model simulations.

For sedimentation (case f), we initialize with an existing rain water layer between 5500 and 7000 m, similar to what was done in Milbrandt and McTaggart-Cowan (2010), the only difference being that our initial rain water

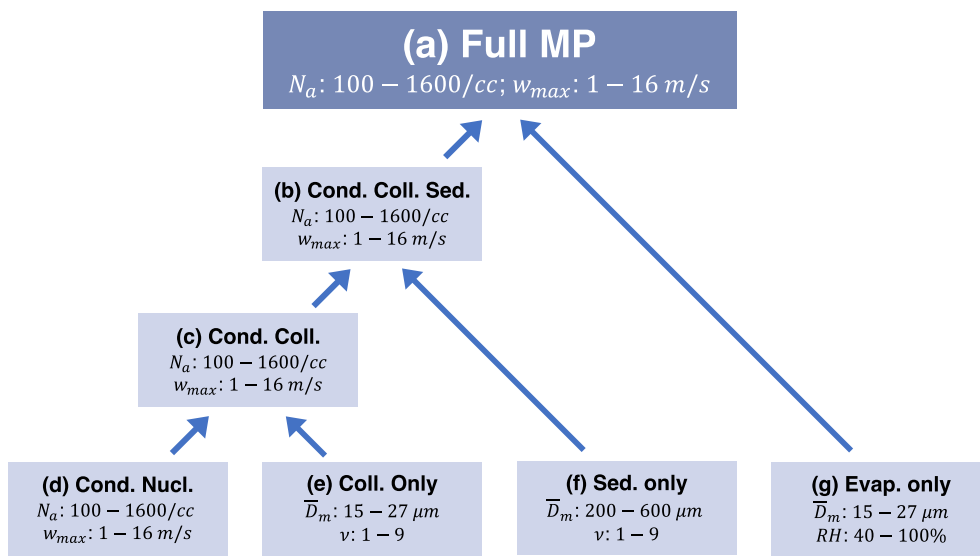

Figure 3. A selection of simulations tested in this study. Note that all cases with condensation turned on automatically include the nucleation process and it is found to lead to almost no difference between AMP and bin schemes.

path increases linearly from 0 at the bottom to 0.5 g/kg at the top of the layer. The $\overline{D}_m$ in these cases are set to typical raindrop sizes ($200-600\,\mu$m). As with collision-coalescence, we vary the shape parameter ($\nu = 1-9$) to test how AMP responds to different initial distribution widths in these idealized cases and there is no vertical wind.

For evaporation (case g), the simulations are again initialized with a liquid water layer between 600 and 1200 m with the same range of cloud droplet sizes as for collision-coalescence. We also vary the initial maximum relative humidity ($RH_{\max}$) from 40% to 100% (Figure 2b). The vertical wind speed evolves according to the yellow dashed line in Figure 2a where $w_{\max} = 2$ m/s. Although there exist countless other combinations of microphysical processes and initial conditions, we find these seven cases to be the most useful for illustrating the structural differences between bulk and bin schemes.

4. Differences Between AMP and Bin Simulations

As our main objective is to reveal the structural differences between bulk and bin schemes in general, the results shown in this section (percent differences, coefficients of determination R^2, etc.) compare AMP simulations with simulations using AMP's underlying bin scheme, as was done in I19 and I22. (We note that the bin scheme simulations should not be treated as benchmark or truth, and bin schemes are not inherently superior than bulk schemes in general as the difference between the two bin schemes tested can be significant.) In this study, we run AMP with two different underlying bin schemes (SBM and TAU) and we only draw conclusions if a qualitatively similar difference is present for both SBM and TAU.

Figure 4 (hereafter referred to as the pyramid figure) gives a high-level summary of AMP-bin mean differences in the test cases shown in Figure 3. The rest of this section will specifically discuss the full microphysics case regarding an overall AMP-bin difference, cases with individual processes turned on regarding the source of that difference, and the cases along the left edge regarding the interaction effect of microphysical processes on AMP-bin difference.

4.1. Full Microphysics

For the full microphysics simulations, we compared several cloud/precipitation properties between AMP and bin and here we show three: liquid water path (LWP), cloud water path (CWP), and surface precipitation rate (Figure 5). There are many ways to compare the output of AMP and bin; here we report the correlation of each property's timeseries in AMP with its timeseries in bin in terms of R^2 (text color) and the ratio of each property's temporal mean in AMP to that in bin (cell shading). Overall, we find similar LWP between AMP and bin but very different CWP and surface precipitation rate.

The cloud property that is most similar between AMP and bin is LWP. We find that the difference in LWP between bin and AMP is small across the simulation suite for both underlying bin schemes, with a mean ratio between 0.9 and 1.1 (or percent difference less than 10%) (Figures 4a, 5a, and 5b). This is expected because LWP is strongly controlled by condensation, which behaves similarly between the AMP and bin schemes (see Section 4.2.1), despite AMP having no knowledge about the explicit distribution from the previous time step.

On the other hand, the two schemes start to diverge when it comes to the partitioning of liquid water content into cloud and rain water content. Across the entire simulation suite, AMP consistently underestimates the rain water content (Figure 4a) and overestimates cloud water (Figures 4a, 5c, and 5d), each by ~20% on average. As we will show, this discrepancy likely comes from the collision-coalescence process. As the derivative of cloud droplets, raindrops can be inherently harder to predict in AMP even with the same physical parameterization as the bin model. The biggest difference between AMP and bin lies in their mean surface precipitation rate, where AMP predicts consistently less rainfall than the bin counterpart by at least 10%, sometimes up to 50% (Figures 4a, 5e, and 5f). This is because surface precipitation is sensitive to not only the aforementioned rain production rate but also sedimentation rate, which is another process that leads to an even larger difference between the two schemes (see Section 4.2.3). Finally, differences in cloud droplet and raindrop number concentration are inconsistent in sign across the AMP-bin pairs, but usually 10% or less (Figure 4a).

Despite the noticeable difference between AMP and bin schemes, it is also worth noting that the magnitude of the AMP-bin difference is similar to that between the two bin schemes, TAU and SBM, as shown in a times series comparison of cloud water path and mean surface precipitation rate in Figures 6a and 6b for the case $N_a = 400$/cc, $w_{\max} = 2$ m/s. Figures 6c and 6d summarizes the full simulation suite similarly to Figure 5. The important implication from this significant TAU-SBM difference is that, when comparing cloud water path and mean surface precipitation, the parameterization differences (between TAU and SBM) are at least as important

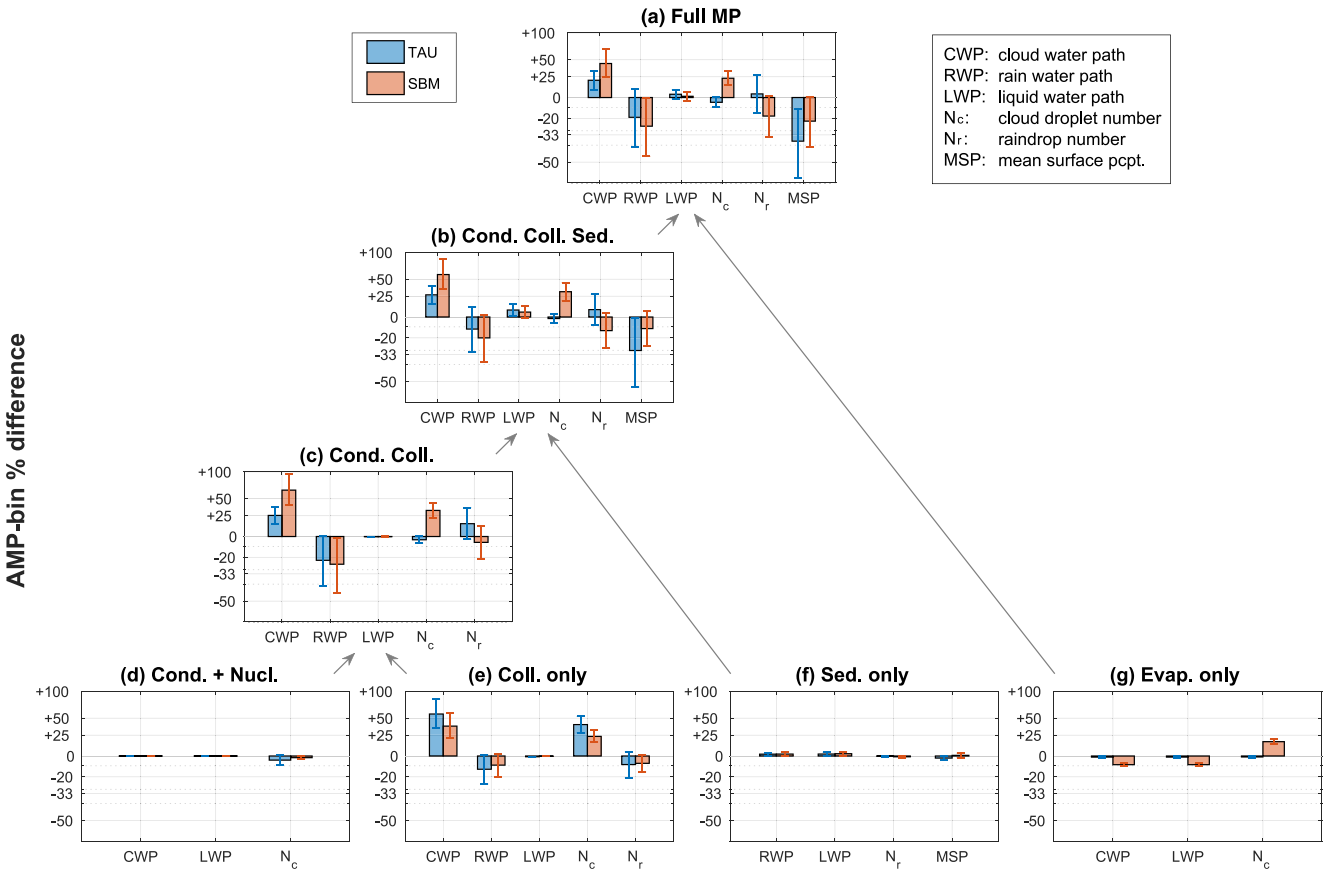

Figure 4. Summary of the effect of structural difference between AMP and bin. Each bar represents the mean percent difference between AMP and bin across the simulation suite shown in Figure 3, with the error bar showing the standard deviation of AMP-bin ratio across the initial condition space. The vertical axes are in log-scale for intuitive ratio comparison. Variable symbols are defined in the upper-left box.

as the structural differences (between bin and bulk schemes), if not more important in the case of TAU. This suggests that it is difficult to draw any conclusions about the ways in which bin schemes are "better" than bulk schemes by simply comparing off-the-shelf bin and bulk schemes.

In summary, across the entire aerosol concentration ($100 - 1600/\text{cc}$) and maximum vertical velocity ($1 - 16\,\text{m/s}$) domain, we find that the overall AMP-bin difference is small and usually even less prominent than the difference between the two underlying bin schemes (SBM and TAU).

4.2. Simple Microphysics

In order to understand which microphysical process(es) most contribute to the manifestation of structural differences between the scheme types, we next discuss the idealized simulations with only single microphysical processes (condensation and nucleation, evaporation, sedimentation, and collision-coalescence).

4.2.1. Condensation and Nucleation

When only condensation and nucleation are turned on, our tests show that AMP can capture the evolution of cloud mass almost perfectly regardless of aerosol concentration or vertical velocity while it slightly underestimates number concentration compared to the bin schemes (Figure 7). Among the 25 test cases, only one case ($N_a = 400/\text{cc}$; $w_{\max} = 4\,\text{m/s}$) will be shown in detail since all cases in the simulation suite are qualitatively similar and the magnitude of the difference is not a function of the initial conditions.

For cloud mass, the nearly perfect emulation of the bin scheme suggests that having the knowledge of the explicit PSD is not necessary for predicting the cloud water path when condensation is the dominating microphysical process in a cloud. This is perhaps not surprising since the amount of mass condensed is largely a product of

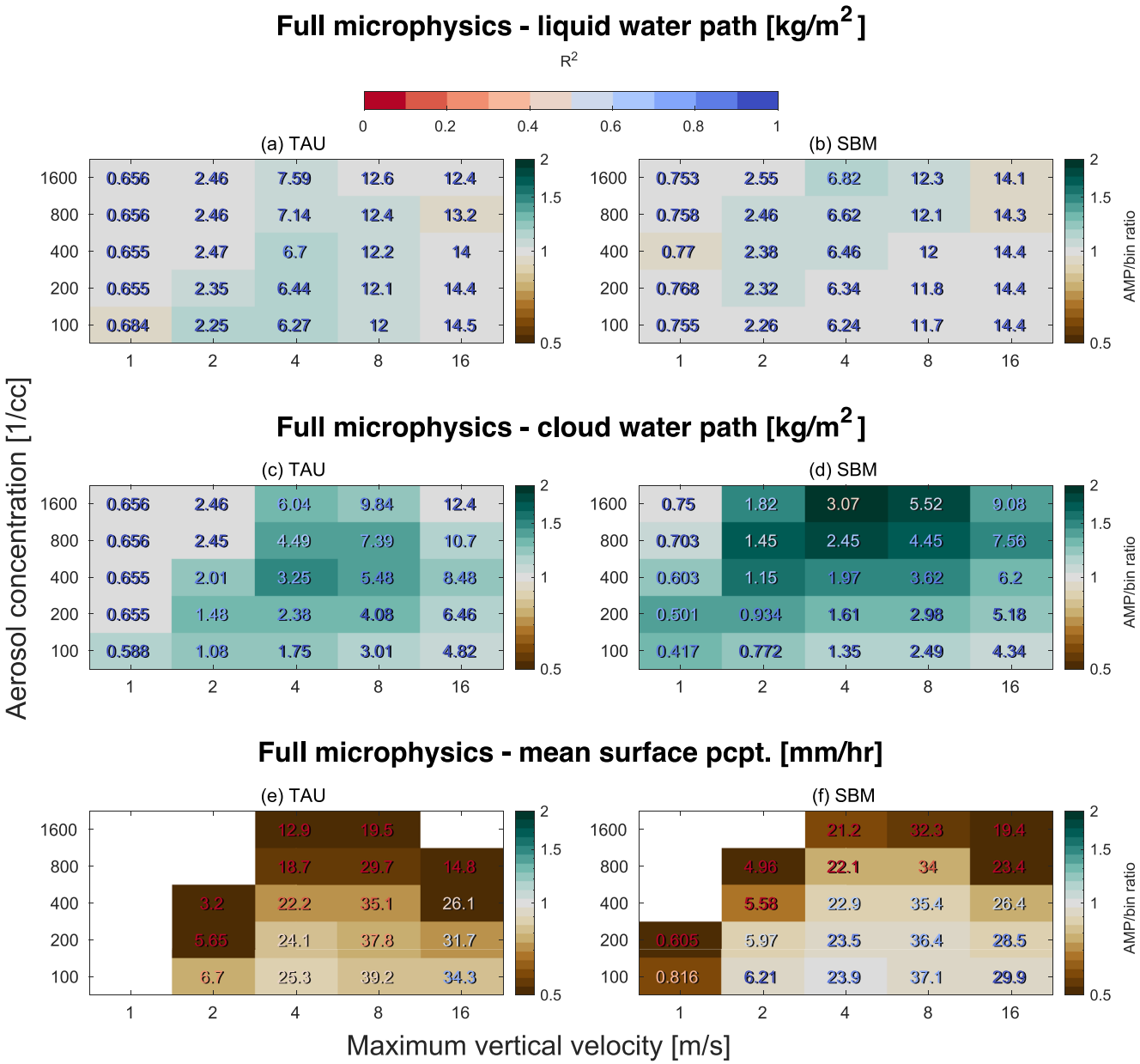

Figure 5. Summary of how mean (a, b) LWP, (c, d) CWP, and (e, f) mean surface precipitation are sensitive to aerosol concentration and maximum vertical velocity. Bluer numbers and grayer grid cells mean more similarity between AMP and bin simulations. Each grid cell represents a full simulation with a certain combination of aerosol concentration and vertical velocity. Number in the grid: the mean value of, for example, LWP across the entire bin simulation. Color of the number (red-blue): temporal correlation (R^2) between AMP and bin. Grid cell shading (brown-green): ratio of mean value of, for example, LWP (AMP/bin).

the evolution of supersaturation, which is strongly controlled by the dynamics but only weakly affected by the microphysics routine of the simulation.

With regard to the number concentration, the AMP-bin difference is slightly larger (Figure 7a) but still largely insignificant compared to the differences from other microphysical processes (Figure 4d). This difference is not related to condensation but due to droplet activation and the constraint of an assumed gamma distribution. Bin schemes typically activate a certain number of droplets based on CCN concentration and supersaturation and then assign them with the smallest possible diameter. This results in a discrete distribution with all droplets in one size bin. According to Steps 1 and 2 of the AMP procedure (Figure 1), AMP has to fit a gamma distribution to that one-bin histogram and then discretize it while ensuring mass conservation before passing the discrete distribution into the bin microphysics routine. However, the Step 1 of the AMP procedure might fail when no combination of

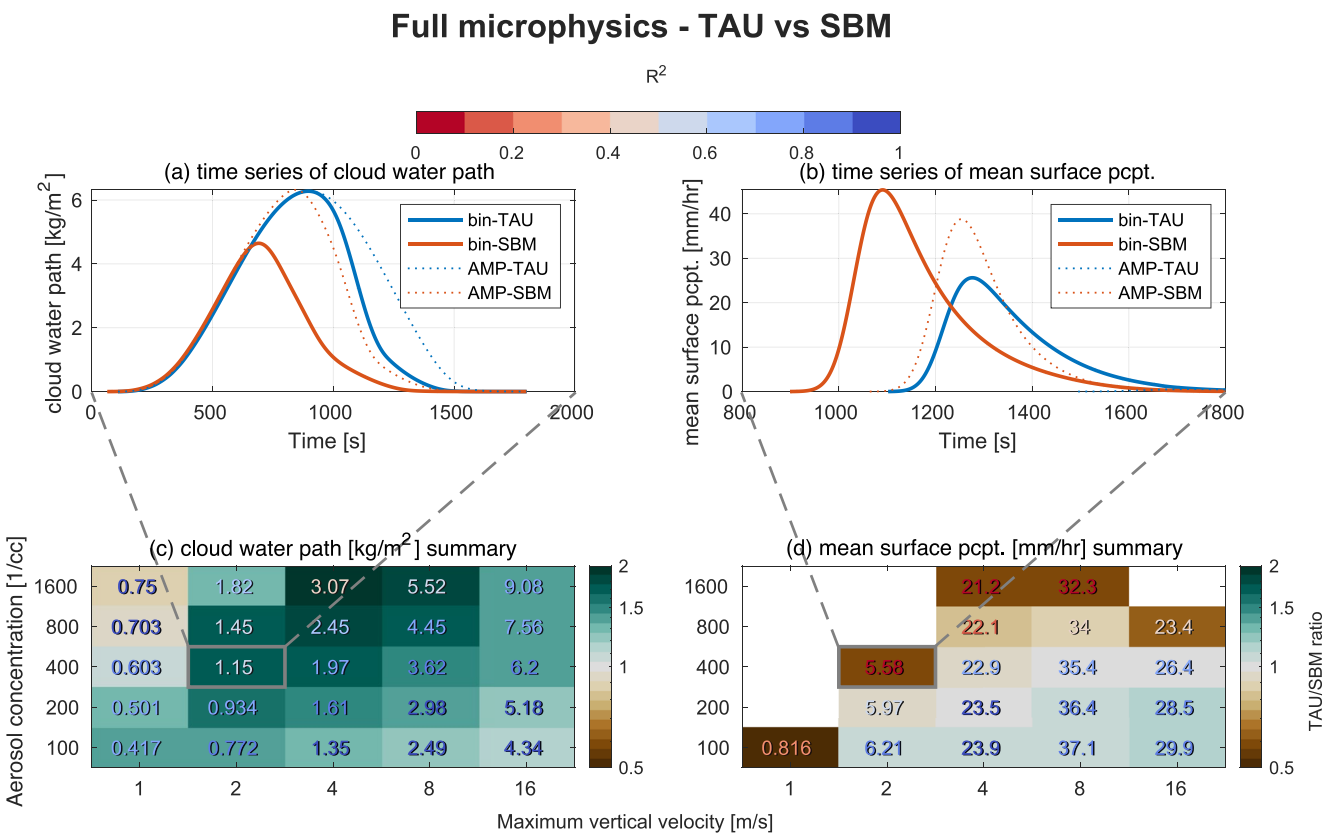

Figure 6. Time series of (a) cloud water path and (b) mean surface precipitation rate of the case $N_a = 400/\text{cc}$, $w_{\max} = 2\,\text{m/s}$. A summary comparison between TAU and SBM is shown in (c) cloud water path and (d) mean surface precipitation rate, which is similar to Figures 5c–5f. The number in the grid is now the mean value of the corresponding variable in the entire SBM simulation. The grid cell shading represents the ratio of mean value between TAU and SBM.

gamma parameters can be found to conserve all three moments (3rd, 0th, 6th) in which case small differences are introduced for the 0th and 6th moments but not the 3rd moment (by design). The time and altitude of such failure are shown in red in Figure 8b, and one such instance is zoomed in and shown in Figure 8a. As noted earlier, the bin scheme's (SBM) distribution has all mass in the smallest size bin, whereas AMP overflows a small portion to the larger size bins due to the constraint of a gamma distribution. Since mass is always conserved during Step 1 of the AMP procedure, this leads to an overestimation of mean droplet size and therefore an underestimation of number concentration. Although AMP can sometimes fail to represent the bin scheme during droplet activation, in reality, however, newly activated droplets do not all have the same size. Compared to bin schemes in which all

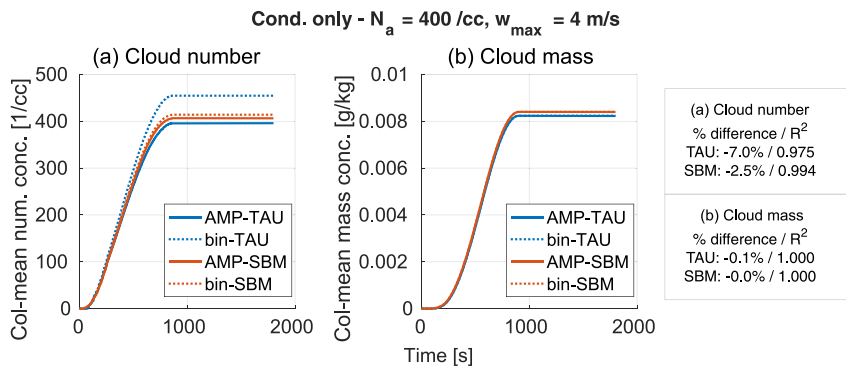

Figure 7. Evolution of column-mean cloud droplet (a) number and (b) mass concentration. The mean AMP-bin percent difference of all 25 tested cases and their R^2 are noted on the rightmost panel.

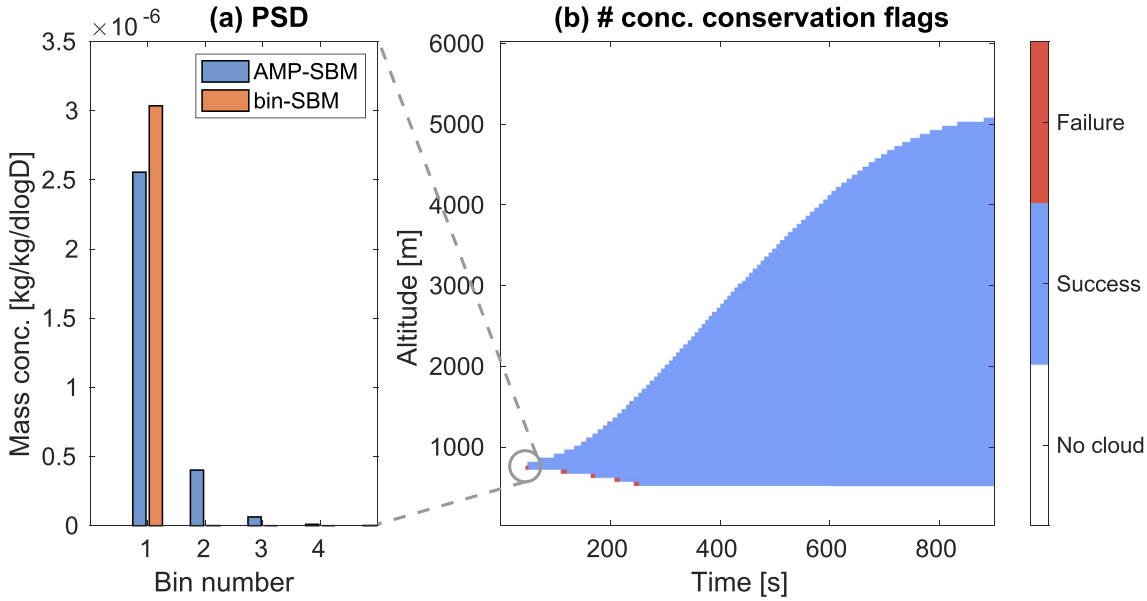

Figure 8. (a) A snapshot of PSD at $t = 45\,s$, $z = 750$ m (circled in b). Only the first four bins are shown since the rest have no mass. (b) Profile of whether number concentration conservation is successfully conserved during Step 1 of AMP procedure. Only the first half (900 s) of the simulation is shown since no new droplets are activated in the second half. Note that mass again is always conserved.

newly activated droplets are of the same size, which results in a zero-width PSD, the bulk approach that uses a gamma distribution to describe the PSD of newly activated droplets is perhaps closer to reality.

I19 also found that AMP could nearly perfectly reproduce the bin results for condensation alone. However, in those tests, droplet nucleation was not included, and AMP and bin simulations always started with identical droplet size distributions. As such, the tests here provide a more rigorous test of AMP's ability to simulate the condensation rates by adding in the complexity of droplet nucleation.

4.2.2. Evaporation

We find negligible difference between AMP and bin schemes for the evaporation-only simulation suite with varying initial cloud droplet sizes and relative humidity (RH) environments. AMP-SBM tends to evaporate mass too quickly but reduce the number concentration too slowly compared to bin-SBM (Figure 4g). AMP-TAU and bin-TAU are nearly identical (Figure 4g). There was no strong dependence of the differences on the initial RH or initial mean droplet size. As with the condensation only case, only one simulation will be shown in detail due to the similarity between all test cases. Figure 9 shows the evolution of cloud number and mass for the case $RH = 99\%$, $\overline{D}_m = 25\,\mu$m. Although AMP and bin somewhat diverge when the fraction remaining is between 0.1 and 0.7, the overall difference between AMP and bin is small (<10%) and comparable to, if not smaller than, the difference between bin-SBM and bin-TAU.

The reason why AMP tends to evaporate number more slowly and evaporate mass faster than the bin schemes is likely because of the homogeneous mixing assumption in which all droplets are assumed to experience the same relative humidity. As shown in the snapshots of size distribution in Figure 10, as evaporation eliminates smaller droplets faster than larger droplets, the mean droplet size increases and the distribution shape changes for the bin scheme case. On the other hand, since AMP is forced to let the distribution shape conform to a gamma one, it redistributes mass within the PSD and inadvertently creates droplets even larger than before the evaporation, as shown in the shaded areas in Figure 10. This behavior is especially evident in AMP-SBM. These handful of extra-large droplets are what lead to the slower number evaporation and faster mass evaporation shown in Figure 9. Nevertheless, since this effect is not present in TAU, we can conclude that this problem is not universal to bulk schemes in general and can be largely mitigated with an appropriate parameterization for evaporation.

We tested evaporation of rain ($\overline{D}_m = 200 - 600\,\mu$m) in addition to cloud with the four schemes and found no difference between AMP and bin since the aforementioned effect becomes negligible when the mean size is significantly larger (not shown).

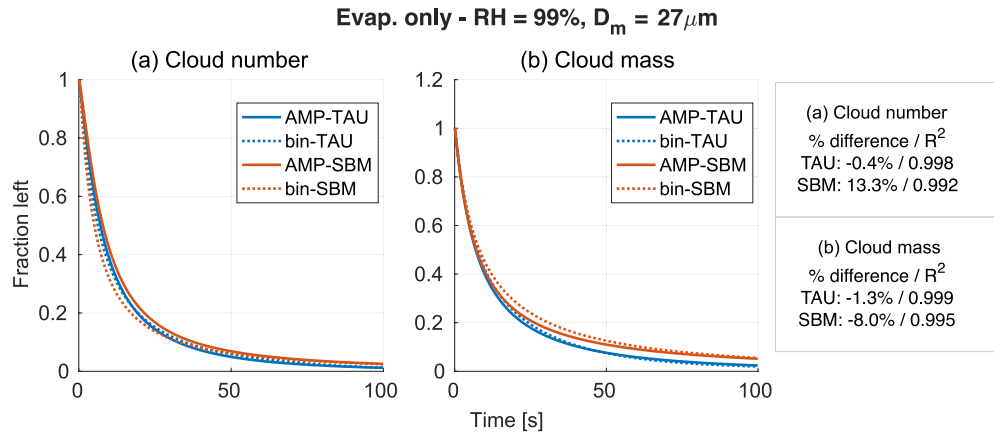

Figure 9. Fraction of (a) cloud number and (b) cloud mass evaporated over time with 99% initial maximum RH, 25 μm $\overline{D}_m$. The shape parameter is set to 4, and the mass mixing ratio is set to 1 g/kg. The mean AMP-bin percent difference of all 25 tested cases and their R^2 are noted on the rightmost panel.

4.2.3. Sedimentation

The sedimentation-only simulation suite tests how raindrop PSDs with different mean sizes and distribution widths respond to sedimentation. AMP is found to have a slightly less size-sorting effect than the bin schemes. However, the mean AMP-bin difference is found to be small (<5%) for both rain mass and number concentration (Figures 4f and 11). Like the previous two tests, one representative case ($\overline{D}_m = 600\ \mu$m, $\nu = 3$) will be shown in detail below since the results are similar across cases. As can be seen in Figure 12, the evolution of rain mass and number can be captured reasonably well by AMP, while it tends to overestimate the sedimentation rate of rain number and underestimate the sedimentation rate of rain mass compared to bin schemes. A detailed comparison between the PSDs of AMP and bin can be seen in Figure 13. This AMP-bin difference is likely again due to the constraint of an assumed distribution shape. Since the largest droplets preferentially fall from the layers above, the PSD of the layers below starts to become less gamma-like due to these additional largest droplets. Again, as AMP does not remember the explicit PSD between time steps, the mass of these largest droplets that fell to the layers below in the previous time step is redistributed toward droplets of smaller sizes. As terminal velocity is positively correlated with droplet size, the artificial loss of these largest droplets leads to a lower sedimentation rate, which manifests as a slightly weaker size sorting effect compared to the bin schemes, that is, mass falls slower while number falls faster in AMP than the bin schemes. Our results are qualitatively in agreement with Milbrandt and McTaggart-Cowan (2010) who performed similar tests.

4.2.4. Collision-Coalescence

Collision-coalescence in AMP produces rain much more slowly than in the bin schemes, which turns out to be the most difference-inducing microphysical process among all, as was also the case in I19. I22 took a more in-depth

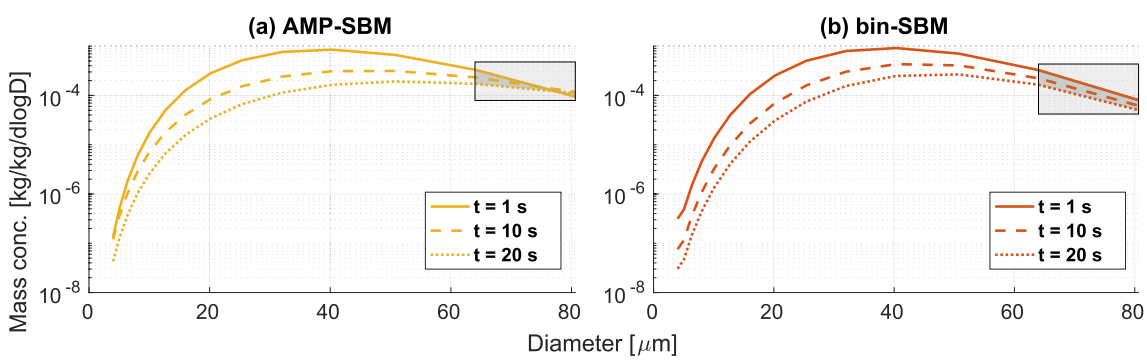

Figure 10. PSD of AMP-SBM versus bin-SBM in the same evaporation simulation as Figure 9 at 1, 10, and 20 s and $z = 1200$ m. The TAU cases are not shown as the difference between AMP and bin is negligible.

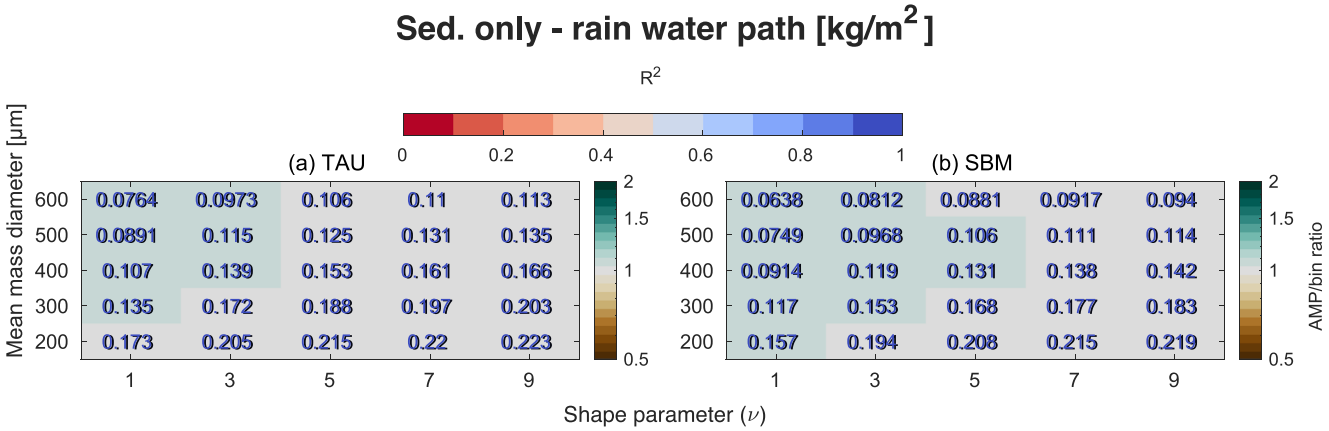

Figure 11. As in Figure 5 but for rain water path in the sedimentation only case.

look at collision-coalescence in AMP versus bin. The results here focus only on the traditional 3M AMP configuration and are in agreement with the discussion in I22.

A comparison of how long it takes for each scheme to convert half of initial cloud mass to rain mass (cloud half-life) through collision-coalescence is shown in Figure 14. AMP is found to be systematically slower than the bin schemes at growing cloud droplets into the rain category. A closer look at the comparison of the PSD evolution reveals that AMP, having two separate cloud and rain modes, often has trouble making "rain initiators," the handful of extra-large droplets that can serve as the seeds for collision-coalescence and the subsequent rain production. Specifically, in the bin schemes, the growth of cloud droplets happens disproportionally to the largest ones between $t = 1$ and 6 min, as indicated by the shaded area in the lower panel of Figures 15c and 15d. Meanwhile, the change in the AMP PSD happens much more evenly across the spectrum, as shown in the upper panels of the same figure (a, b). This behavior of AMP is what delays the production of those rain initiators, and the problem is exacerbated when the condition is not in favor of collision-coalescence, that is, small mean droplet size and large shape parameter, hence the larger discrepancy between AMP and bin toward the lower right corner of Figure 14. The gamma distribution assumption and the intrinsic positive feedback nature of collision-coalescence (more large droplets lead to larger difference in terminal velocity, hence more collisional growth) are the two major factors slowing down the collisional rate in AMP.

Next, we shift our perspective to the differences between AMP and bin in simulating rain production, which is closely related to collision-coalescence. In traditional bulk schemes, warm phase collision-coalescence is artificially

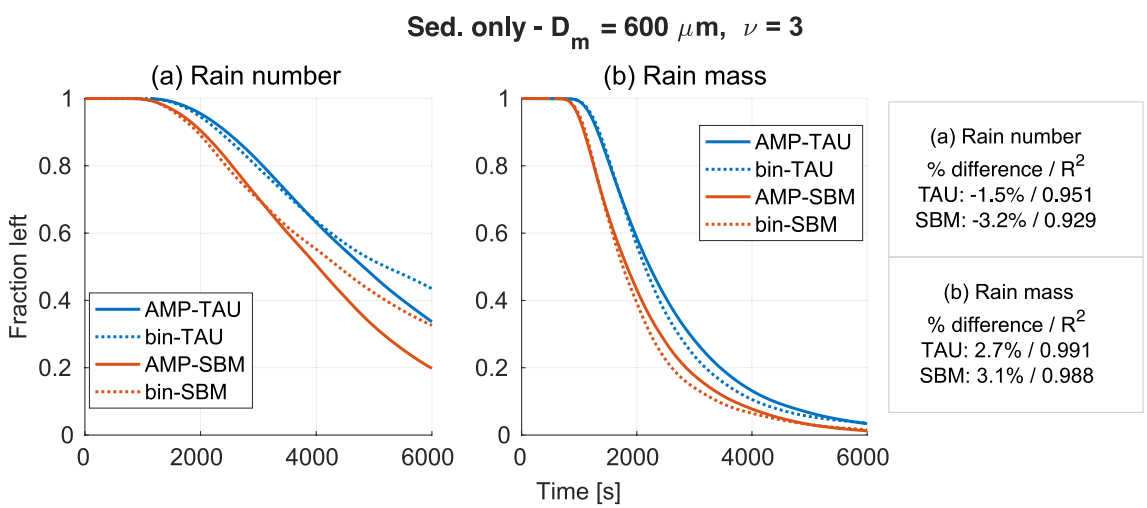

Figure 12. Fraction of (a) rain number and (b) rain mass that has yet to fall out of the system. The mean AMP-bin percent difference of all 25 tested cases and their R^2 are noted on the rightmost panel.

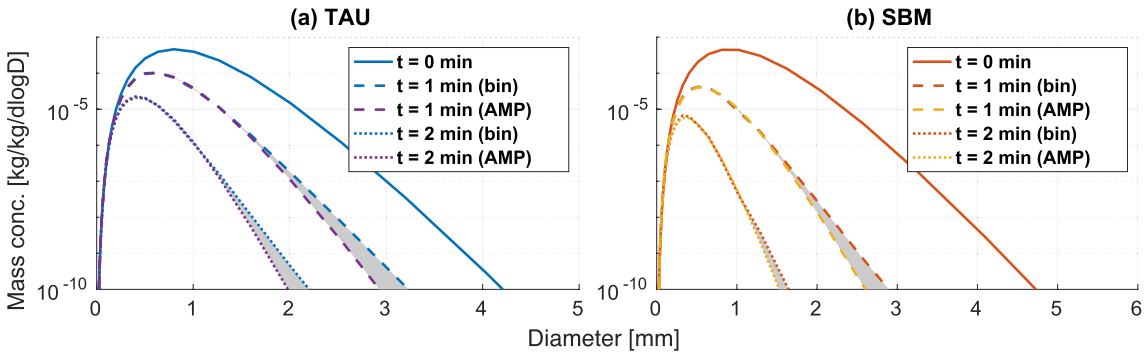

Figure 13. PSD of AMP versus bin in the same sedimentation simulation as Figure 12 at $t = 0, 1, 2$ min. The snapshot is taken at the second to top layer ($z = 6933$ m).

partitioned into three subprocesses: autoconversion (coalescence between cloud-sized droplets to form rain-sized drops), accretion (raindrops collecting cloud-sized droplets to form larger raindrops), and self-collection (of cloud or rain drops). Among them, autoconversion is particularly difficult to model and has posed major challenges to the development of bulk schemes ever since its inception despite the tremendous amount of effort in recent years even with machine learning techniques (Berry & Reinhardt, 1974; Chiu et al., 2021; Graham; Feingold et al., 1998; Khairoutdinov & Kogan, 2000; Kogan, 2013; Lee & Baik, 2017; Liu & Daum, 2004; Seifert & Beheng, 2001; Seifert & Rasp, 2020). In AMP, although the microphysics routine itself is performed by the bin schemes and hence does not distinguish between these modes of collision-coalescence, we can still assess these processes using careful tests.

To see whether the challenge in representing autoconversion in bulk schemes is simply a result of its microphysical parameterizations or its bulk-like structure, we test how the AMP-bin difference is sensitive to the proportion of autoconversion in rain production by initiating a bimodal distribution (two gamma combined) with varying configurations of the two modes. Here, we denote these two modes as the $L1$ mode and the $L2$ mode ("L" for liquid water), where the mean size of $L1$ is smaller than $L2$. Note that the two modes do not imply their respective size being larger or smaller than the cloud-rain size threshold D_t. In the context of collision-coalescence, they can be pictured as the collected mode ($L1$) and the collector mode ($L2$). In all autoconversion sensitivity tests, we set a constant $\overline{D}_m = 15\ \mu$m for the $L1$ mode, a constant total liquid water content at $q_l = 1$ g/kg, same initial $\nu = 5$ for both $L1$ and $L2$ modes, but vary mass fraction of the collector $L2$ mode ($X_{L2} = \frac{L2\ \text{mass}}{L1\ \text{mass}+L2\ \text{mass}}$) from 10^{-5} (almost all $L1$) to 1 (all $L2$) and a varying initial mean mass diameter of the $L2$ mode ($\overline{D}_{L2m}$) from 30 μm to 100 μm. If AMP can perform autoconversion well, then perhaps autoconversion parameterizations in bulk schemes can be improved. If AMP *only* has trouble in the cases where autoconversion dominates the rain production (high X_{L2} and low $\overline{D}_{L2m}$) but not in others, then we can conclude that the autoconversion problems in bulk schemes are not a result of poor autoconversion parameterizations but rather the structure of AMP-like bulk schemes.

The upper panels of Figure 16 show how much AMP and bin diverge as a function of X_{L2} (with a constant $\overline{D}_{L2m} = 50\ \mu$m) and as a function of $\overline{D}_{L2m}$ (with a constant $X_{L2} = 10^{-3}$). Clearly, AMP-bin difference is the largest when autoconversion dominates rain production (low $L2$ mass fraction and small $L2$ mode $\overline{D}_m$). This result shows that AMP and bin perform very similarly for accretion, but differently for autoconversion, which suggests that the difficulty in representing autoconversion is likely due to the bulk-like structure rather than the parameterization.

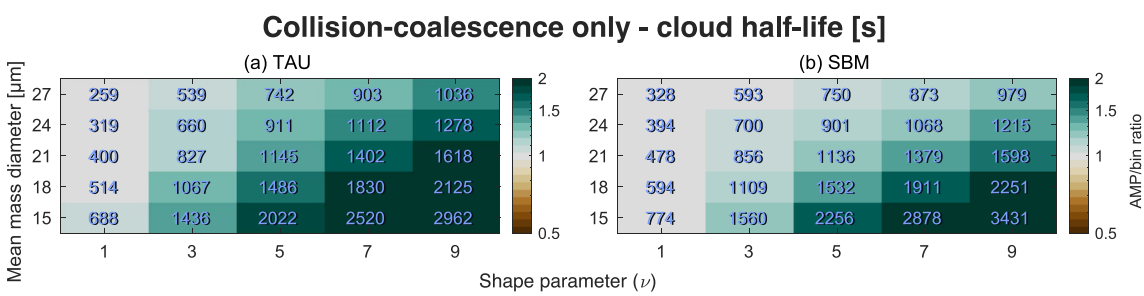

Figure 14. As in Figure 5 but for cloud half-life in collision-coalescence only simulations.

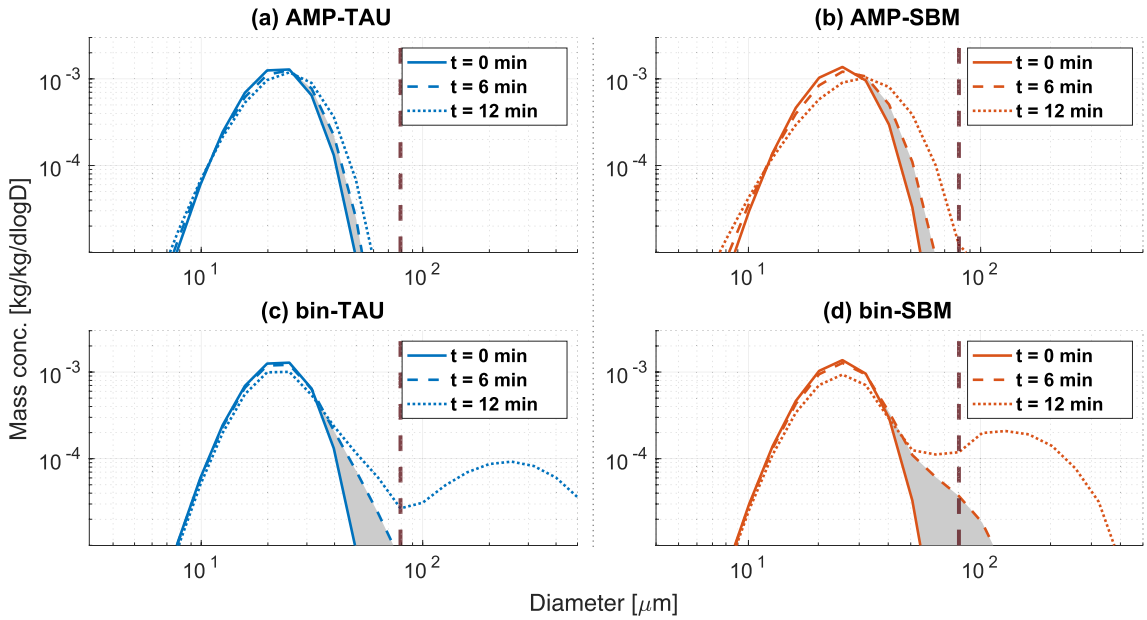

Figure 15. Snapshots of size distribution for AMP and bin schemes in the collision-only simulation ($\overline{D}_m = 21\ \mu$m, $\nu = 9$, $z = 1200$ m). The shaded area represents the change in distribution between 1-min and 6-min mark. The dark red vertical dashed line marks the threshold size separating cloud and rain category in AMP.

Almost all existing bulk schemes, however, are not only moment-resolved and have a fixed distribution shape, they typically also feature an artificially separate liquid water category (cloud mode vs. rain mode). To test whether the representation of autoconversion is susceptible to this common feature of bulk schemes, we then perform the same set of tests using a version of AMP with a unified liquid water category, in which AMP searches for two sets of gamma parameters at the same time to create a bimodal distribution that conserves the total liquid water content (Step 1 of Figure 1), instead of sequentially searching for the gamma parameters for each liquid water categories (details of its mechanics can be found in I22). The lower panels of Figure 16 show the advantage of this AMP configuration. With the exact same microphysics routines and underlying moment-resolved structure as the original AMP, the unified category AMP is much better at representing the underlying bin schemes in almost all test cases, especially for cases where the original AMP struggles the most (high X_{L1} and low $\overline{D}_{L2m}$).

These results suggest that the perennial challenges involving autoconversion in bulk schemes likely stem not from the moment-resolved structure of a bulk scheme, but the fact that liquid water is artificially separated into two categories. If future studies can verify this finding with more general and realistic initial model configurations, then a bulk scheme with a unified liquid water category can potentially be more realistic than a traditional bulk scheme. I22 also found that the predefined cloud-rain size boundary could also slow down the growth of cloud droplets into the rain category, and the difference can be greatly reduced when AMP is configured to have a unified bimodal liquid category. For detailed analysis of collision-coalescence, we refer the interested readers to I22.

4.3. Interaction Effects Between Processes

The pyramid figure (Figure 4) summarizes how the structural difference between AMP and bin manifests as microphysical processes are progressively combined. Each bar represents the average percent difference between AMP and bin across a simulation suite designed for each process combination (shown in Figure 3).

An important suggestion from this pyramid figure is that the effect of structural differences in the full microphysics case (Figure 4a) can be traced down to the collision-coalescence (Figure 4e), suggesting that collision-coalescence is the major source of disagreement between AMP and its bin counterpart. Remarkably, the magnitude of the differences in the full microphysics simulations (Figure 4a) are nearly always of the same sign and of similar magnitude to those in the case of collision-coalescence only (Figure 4e).

It is most meaningful to trace the differences along the left edge (case d → c → b → a) since these simulation suites all use the same set of initial conditions. Figure 17 shows the change in AMP-bin percent difference by adding

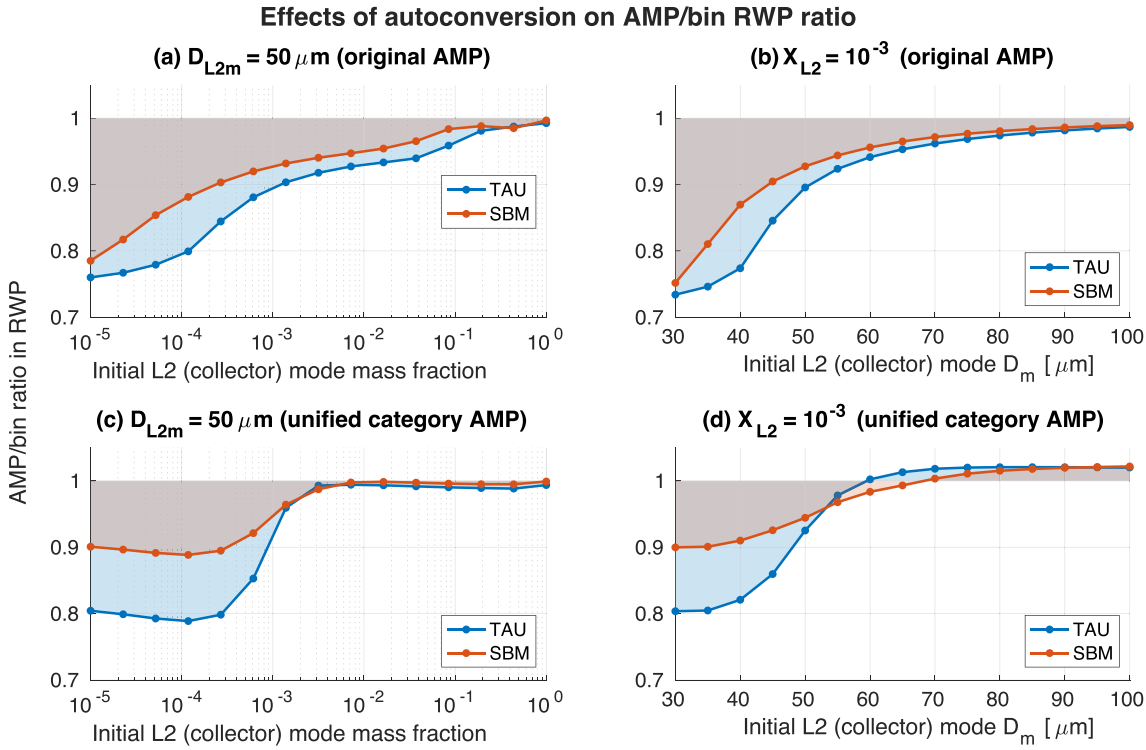

Figure 16. AMP/bin ratio in RWP as a function of initial L2 (collector) mode mass fraction and L2 mode $\overline{D}_m$. The upper panels are from the original AMP (with two liquid categories), and the lower panels are from the single category AMP (bimodal gamma). The shaded area shows the difference between AMP and its target (AMP/bin = 1).

the process of sedimentation and evaporation to the simulation. The most noticeable change when sedimentation is added (case c to case b) is a slight increase in the LWP difference. This difference in LWP though is reduced in the full microphysics simulations (case a) when evaporation is added. In fact, for most quantities in Figure 19, the changes due to the addition of sedimentation are opposed by the addition of evaporation. These results suggest that the interaction of microphysical processes does not serve to amplify differences between AMP and bin, but rather that the interaction of processes, at least in this idealized scenario, has a small or insignificant impact on the total differences for most cloud and rain properties in AMP.

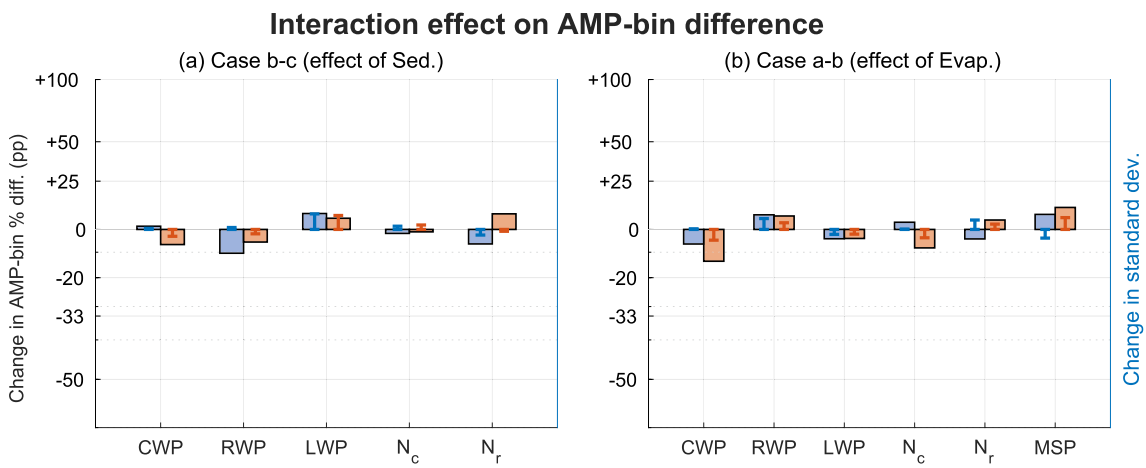

Figure 17. Effect of adding a microphysical process on AMP-bin difference. Bar heights represent the change in AMP-bin difference in percentage points (pp). Error bars represent the change in standard deviation by adding the process. The vertical axis range is kept the same as Figure 4 for intuitive comparison.

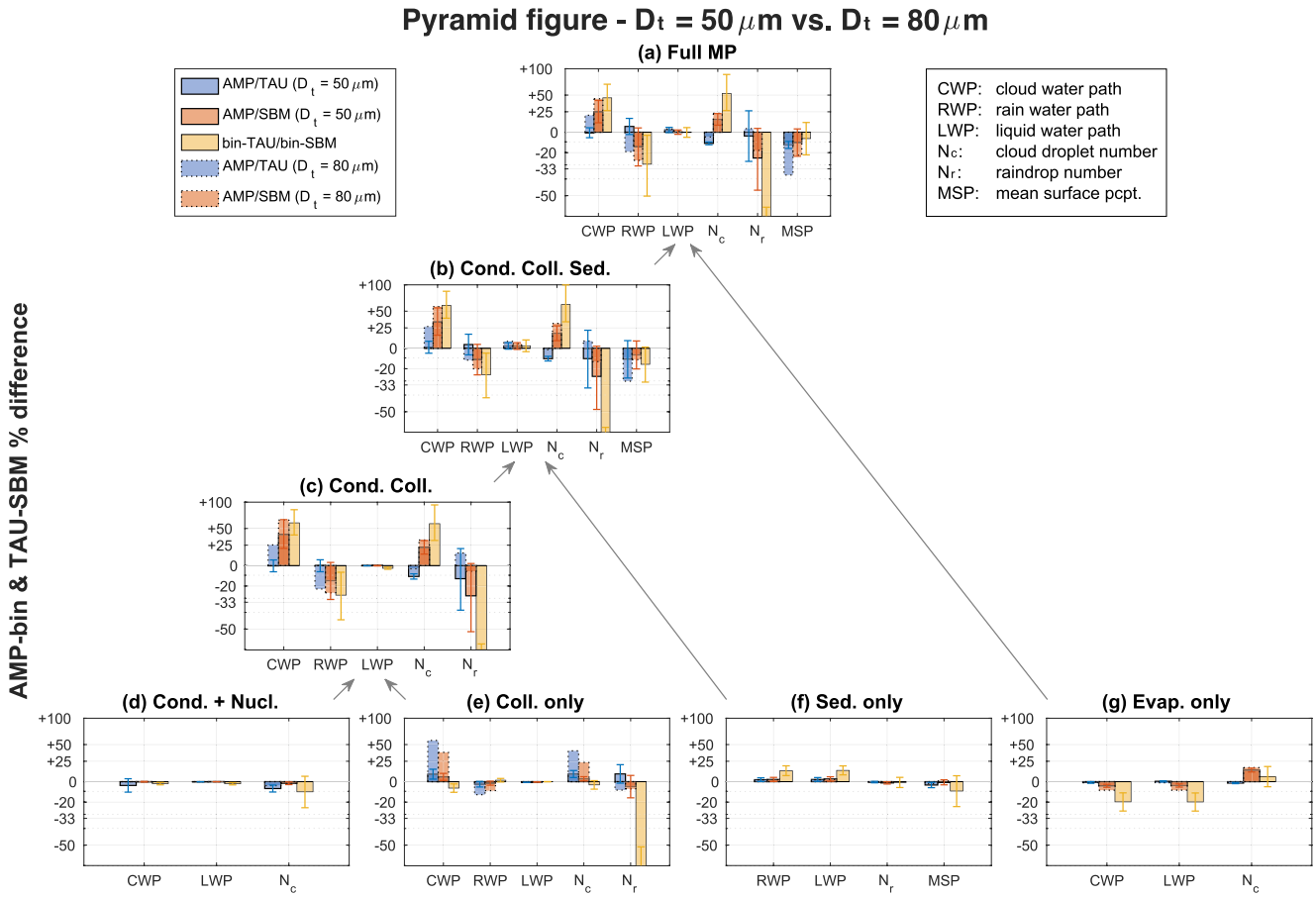

Figure 18. A pyramid figure comparing the AMP-bin difference between $D_t = 50\ \mu$m (solid border) and $D_t = 80\ \mu$m (dotted border, same as Figure 4) as well as the TAU-SBM difference. The error bars represent the standard deviation of AMP-bin or TAU/SBM ratio across the initial condition space.

4.4. Alternative Size Threshold Separating Cloud Droplets and Raindrop

Since AMP has cloud and rain as separate liquid water categories, one parameter that could affect the autoconversion rate in AMP is the size threshold separating the two categories. A lower size threshold could lead to faster autoconversion due to an earlier emergence of the rain mode, which can help mitigate the slow rain production problem associated with collision-coalescence discussed in Section 4.2.4. A smaller size threshold was tested in I22, and it was shown that, for the collision-coalescence process alone, a diameter threshold of $D_t = 50\ \mu m$ can greatly improve AMP's representation of SBM in a box model.

Here we rerun the entire simulation suite (Figure 3) to test the generality of this result by extending the simulation to one-dimensional model (KiD) and two types of bin schemes (TAU and SBM). In agreement with I22, we also find that AMP is much better at reproducing the bin results with this lower size threshold. Figure 18 shows that almost all the cases with $D_t = 50\ \mu$m (bars with solid borders) have a smaller AMP-bin difference than its $D_t = 80\ \mu$m (dotted borders) counterpart, especially for cloud water path and mean surface precipitation. Quite remarkably, the lower threshold results in nearly perfect partitioning of the LWP in AMP-TAU (Figure 17a).

The lower size threshold does occasionally result in larger differences than previously. Most notably, AMP with the lower threshold in case (d), where only condensation and nucleation are turned on, predicts a slightly lower cloud water path in AMP-TAU compared to bin-TAU. A closer look into the individual simulation (Figure 19) reveals that the apparent deficit in cloud water path comes from the early emergence of the rain mode due to the lower D_t, which results in a premature rain production via condensation. Note that the total liquid water condensed is still the same between AMP and bin, as shown in Figure 18d (LWP).

Nonetheless, the overall effect of this lower $D_t = 50\ \mu$m is clearly a net positive over the original $D_t = 80\ \mu$m when full microphysics is turned on. This change puts the AMP-bin difference even lower, often substantially

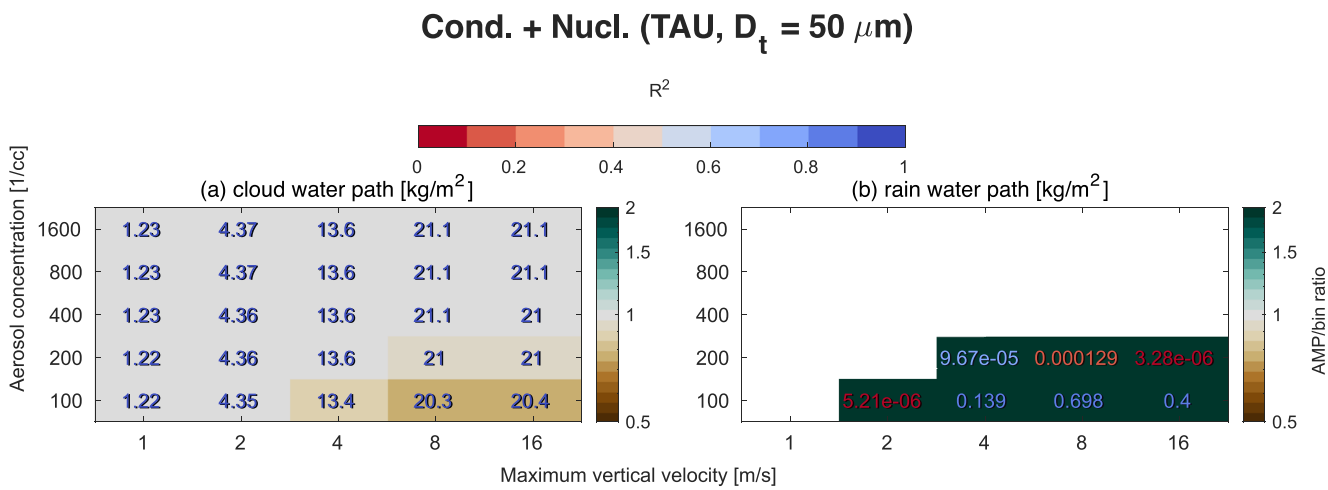

Figure 19. Summary of how (a) cloud and (b) rain water path is sensitive to aerosol concentration and maximum vertical velocity when only nucleation and condensation is turned on. Only TAU is shown in the figure as the AMP-bin difference found in SBM is negligible.

lower, than the TAU-SBM difference (yellow bars in Figure 18), making the effect of structural differences between AMP and bin even smaller than the parameterization differences between the two bin schemes.

5. Summary

This study investigates how the structural differences between bin and bulk schemes (size-resolved vs. moment-resolved) manifest in their simulation results and how that knowledge can help shape the future of bulk scheme development. To do this, we must ensure that the bin and bulk schemes used in this study have identical microphysical parameterization routines, which can be a confounding variable, which is something that previous studies on this topic could not do since existing bin and bulk schemes are also different in their parameterizations. For this study, we use two existing bin schemes (SBM and TAU; Feingold et al., 1988; A. Khain et al., 2004; Tzivion et al., 1987, 1999) as the "benchmarks" and a custom-made bulk scheme (AMP; Igel, 2019), which is a wrapper function for an existing bin scheme. Because AMP uses the parameterization of the underlying bin scheme while only remembering the moment values between time steps (rather than the explicit PSD), it is technically a bulk scheme, and we can compare it against its underlying bin scheme to study the effect of their structural differences.

To build on what was done in Igel (2019), we adapted the 3M AMP into a one-dimensional kinematic driver (KiD) model and designed a suite of simulations with different model complexity. We first run tests with full microphysics turned on (condensation and nucleation, evaporation, sedimentation, and collision-coalescence), and then decompose them into individual and key combinations of processes in order to understand why bin and bulk schemes diverge and to study the interaction effects of microphysical processes on the AMP-bin difference. To make sure that the conclusions apply to a wide range of environmental and dynamics characteristics, we give each case a set of possible initial conditions (see Figure 3). We have the following conclusions based on these simulations:

1. Condensation alone can be represented almost perfectly by AMP compared to its underlying bin scheme, while droplet nucleation may cause AMP to underestimate slightly the number concentration due to the gamma distribution assumption. However, AMP's (or bulk schemes in general) approach could be desirable given that newly-activated droplets do not all fall into one size bin in reality.
2. Evaporation and sedimentation can be well represented by AMP. Small differences (<10%) may be noticeable due to the structural differences, but the AMP-bin difference caused by these processes are mostly negligible.
3. Collision-coalescence is the single largest source of discrepancy when AMP tries to emulate its bin counterpart. More specifically, AMP and bin struggle to agree on the rate of autoconversion but appear to agree well if accretion is the dominant mode of rain production. Rain production in AMP can be significantly slower than the bin scheme when the cloud-rain threshold diameter is 80 μm. However, substantial improvement is gained when the threshold diameter is moved to 50 μm or if a unified liquid category is used (see also I22).

4. When full microphysics is turned on:
   a) Total liquid water content are represented well in AMP, with a mean AMP-bin difference of less than 5% for both quantities, regardless of the initial condition. This is because both quantities are largely controlled by condensation, which AMP can successfully represent as mentioned above.
   b) The quantity that shows the largest AMP-bin difference is the mean surface precipitation. The onset of precipitation predicted by AMP lags behind its underlying bin scheme since it is a product of sedimentation and collision-coalescence, both of which suffer, to a different degree, from the gamma distribution assumption. Again, a lower size threshold improves AMP's performance.
5. The interaction of microphysical processes does not serve to amplify the differences between AMP and bin, but rather has a small or insignificant impact on the total differences for most cloud and rain properties in AMP.

A surprising finding that is worth special recognition is that, in the full microphysics case, the mean AMP-bin difference is at least of the same magnitude of (when $D_t = 80\ \mu$m), and can be substantially smaller than (when $D_t = 50\ \mu m$), the mean TAU-SBM difference regarding cloud water path and surface precipitation rate (Figure 18). This shows that the choice of parameterization (SBM or TAU) can have an impact on the simulation results that is larger than the impact of model structure (bin or bulk). The results overall suggest that bulk schemes, *in principle*, are not as inherently limited in their ability to simulate microphysical processes as has been previously suggested (e.g., Fan et al., 2016). Rather, here we have shown that bin (size-resolved) and bulk (moment-resolved) schemes are more similar than they are dissimilar. In addition, if we look at these results from the opposite angle, the large differences between bin-SBM and bin-TAU show that the inherent uncertainties within the bin schemes can be much more significant than the structural differences between AMP and bin. This stresses that the results from bin scheme simulations should not be interpreted as ground truth by default but rather only a reference.

In summary, the work here is encouraging as it shows that AMP can emulate its underlying bin scheme under a wide range of circumstances, which is promising for future research involving bulk schemes. We have shown that virtually all AMP-bin differences (which again, for most processes are small) arise from assumptions regarding the underlying assumed PDF. Since the assumption of a fixed functional form is not a required feature for bulk schemes, the structural differences between bulk and bin schemes mentioned in this study can potentially be further minimized with smart implementation of schemes that do not rely on pre-defined functional forms for the PSD in the future (Chiu et al., 2021; Morrison, van Lier-Walqui, Kumjian, et al., 2020; Seifert & Rasp, 2020; van Lier-Walqui et al., 2020). Alternatively, as suggested in I22, the use of a unified liquid category could also bring the two scheme types closer together. Work is ongoing to further develop and test the unified category AMP in kinematic and dynamic simulations of clouds.

Data Availability Statement

The AMP simulation data and visualization code can be found at https://farm.cse.ucdavis.edu/~arthurhu/bulk_bin_alike. The source code for the Kinematic Driver can be found at Hill and Lebo (2018).

Acknowledgments
This work is supported by the National Science Foundation through Grant 2025103. We thank Matthew Igel, Hugh Morrison, Sean Santos, and Marcus van Lier-Walqui for helpful comments and discussions regarding the development of AMP. We also thank Jason Milbrandt and one anonymous review for helpful and constructive comments through the review process.

References

Beheng, K. D. (1994). A parameterization of warm cloud microphysical conversion processes. *Atmospheric Research*, *33*(1–4), 193–206. https://doi.org/10.1016/0169-8095(94)90020-5

Berry, E. X., & Reinhardt, R. L. (1974). An analysis of cloud drop growth by collection: Part IV. A new parameterization. *Journal of the Atmospheric Sciences*, *31*(8), 2127–2135. https://doi.org/10.1175/1520-0469(1974)031<2127:aaocdg>2.0.co;2

Chiu, J. C., Yang, C. K., van Leeuwen, P. J., Feingold, G., Wood, R., Blanchard, Y., et al. (2021). Observational constraints on warm cloud microphysical processes using machine learning and optimization techniques. *Geophysical Research Letters*, *48*(2), 1–13. https://doi.org/10.1029/2020GL091236

Falk, N. M., Igel, A. L., & Igel, M. R. (2019). The relative impact of ice fall speeds and microphysics parameterization complexity on supercell evolution. *Monthly Weather Review*, *147*(7), 2403–2415. https://doi.org/10.1175/MWR-D-18-0417.1

Fan, J., Leung, L. R., Li, Z., Morrison, H., Chen, H., Zhou, Y., et al. (2012). Aerosol impacts on clouds and precipitation in eastern China: Results from bin and bulk microphysics. *Journal of Geophysical Research*, *117*(D16). https://doi.org/10.1029/2011JD016537

Fan, J., Wang, Y., Rosenfeld, D., & Liu, X. (2016). Review of aerosol-cloud interactions: Mechanisms, significance, and challenges. *Journal of the Atmospheric Sciences*, *73*(11), 4221–4252. https://doi.org/10.1175/JAS-D-16-0037.1

Feingold, G., Tzivion, S., & Levin, Z. (1988). Evolution of raindrop spectra. Part I: Solution to the stochastic collection/breakup equation using the method of moments. *Journal of the Atmospheric Sciences*, *45*(22), 3387–3399. https://doi.org/10.1175/1520-0469(1988)045<3387:EORSPI>2.0.CO;2

Feingold, G., Walko, R. L., Stevens, B., & Cotton, W. R. (1998). Simulations of marine stratocumulus using a new microphysical parameterization scheme. *Atmospheric Research*, *47*(48), 505–528. https://doi.org/10.1016/S0169-8095(98)00058-1

Hill, A., & Lebo, Z. (2018). Kinematic driver KiD-A. https://doi.org/10.5281/zenodo.7262715

Igel, A. L. (2019). Using an arbitrary moment predictor to investigate the optimal choice of prognostic moments in bulk cloud microphysics schemes. *Journal of Advances in Modeling Earth Systems*, *11*(12), 4559–4575. https://doi.org/10.1029/2019MS001733

Igel, A. L., Morrison, H., Santos, S. P., & van Lier-Walqui, M. (2022). Limitations of separate cloud and rain categories in parameterizing collision-coalescence for bulk microphysics schemes. *Journal of Advances in Modeling Earth Systems*, *14*(6), 1–20. https://doi.org/10.1029/2022ms003039

Johnson, J. S., Cui, Z., Lee, L. A., Gosling, J. P., Blyth, A. M., & Carslaw, K. S. (2015). Evaluating uncertainty in convective cloud microphysics using statistical emulation. *Journal of Advances in Modeling Earth Systems*, *7*(1), 162–187. https://doi.org/10.1002/2014MS000383

Kessler, E. (1969). On the distribution and continuity of water substance in atmospheric circulations. In *On the distribution and continuity of water substance in atmospheric circulations* (pp. 1–84). American Meteorological Society. https://doi.org/10.1007/978-1-935704-36-2_1

Khain, A., Pokrovsky, A., Pinsky, M., Seifert, A., & Phillips, V. (2004). Simulation of effects of atmospheric aerosols on deep turbulent convective clouds using a spectral microphysics mixed-phase cumulus cloud model. Part I: Model description and possible applications. *Journal of the Atmospheric Sciences*, *61*(24), 2963–2982. https://doi.org/10.1175/JAS-3350.1

Khain, A. P., Beheng, K. D., Heymsfield, A., Korolev, A., Krichak, S. O., Levin, Z., et al. (2015). Representation of microphysical processes in cloud-resolving models: Spectral (bin) microphysics versus bulk parameterization. *Reviews of Geophysics*, *53*(2), 247–322. https://doi.org/10.1002/2014RG000468

Khairoutdinov, M., & Kogan, Y. (2000). A new cloud physics parameterization in a large-eddy simulation model of marine stratocumulus. *Monthly Weather Review*, *128*(1), 229–243. https://doi.org/10.1175/1520-0493(2000)128<0229:ANCPPI>2.0.CO;2

Kogan, Y. (2013). A cumulus cloud microphysics parameterization for cloud-resolving models. *Journal of the Atmospheric Sciences*, *70*(5), 1423–1436. https://doi.org/10.1175/JAS-D-12-0183.1

Lee, H., & Baik, J. J. (2017). A physically based autoconversion parameterization. *Journal of the Atmospheric Sciences*, *74*(5), 1599–1616. https://doi.org/10.1175/JAS-D-16-0207.1

Li, X., Tao, W. K., Khain, A. P., Simpson, J., & Johnson, D. E. (2009). Sensitivity of a cloud-resolving model to bulk and explicit bin microphysical schemes. Part I: Comparisons. *Journal of the Atmospheric Sciences*, *66*(1), 3–21. https://doi.org/10.1175/2008JAS2646.1

Lin, Y. L., Farley, R. D., & Orville, H. D. (1983). Bulk parameterization of the snow field in a cloud model. *Journal of Climate and Applied Meteorology*, *22*(6), 1065–1092. https://doi.org/10.1175/1520-0450(1983)022<1065:BPOTSF>2.0.CO;2

Liu, Y., & Daum, P. H. (2004). Parameterization of the autoconversion process. Part I: Analytical formulation of the Kessler-type parameterization. *Journal of the Atmospheric Sciences*, *61*(13), 1539–1548. https://doi.org/10.1175/1520-0469(2004)061<1539:POTAPI>2.0.CO;2

Meyers, M. P., Walko, R. L., Harrington, J. Y., & Cotton, W. R. (1997). New RAMS cloud microphysics parameterization. Part II: The two-moment scheme. *Atmospheric Research*, *45*(1), 3–39. https://doi.org/10.1016/S0169-8095(97)00018-5

Milbrandt, J. A., & McTaggart-Cowan, R. (2010). Sedimentation-induced errors in bulk microphysics schemes. *Journal of the Atmospheric Sciences*, *67*(12), 3931–3948. https://doi.org/10.1175/2010JAS3541.1

Milbrandt, J. A., & Yau, M. K. (2005). A multimoment bulk microphysics parameterization. Part I: Analysis of the role of the spectral shape parameter. *Journal of the Atmospheric Sciences*, *62*(9), 3051–3064. https://doi.org/10.1175/JAS3534.1

Morrison, H. (2012). On the numerical treatment of hydrometeor sedimentation in bulk and hybrid bulk-bin microphysics schemes. *Monthly Weather Review*, *140*(5), 1572–1588. https://doi.org/10.1175/MWR-D-11-00140.1

Morrison, H., & Grabowski, W. W. (2007). Comparison of bulk and bin warm-rain microphysics models using a kinematic framework. *Journal of the Atmospheric Sciences*, *64*(8), 2839–2861. https://doi.org/10.1175/jas3980

Morrison, H., Milbrandt, J. A., Bryan, G. H., Ikeda, K., Tessendorf, S. A., & Thompson, G. (2015). Parameterization of cloud microphysics based on the prediction of bulk ice particle properties. Part II: Case study comparisons with observations and other schemes. *Journal of the Atmospheric Sciences*, *72*(1), 312–339. https://doi.org/10.1175/JAS-D-14-0066.1

Morrison, H., van Lier-Walqui, M., Fridlind, A. M., Grabowski, W. W., Harrington, J. Y., Hoose, C., et al. (2020). Confronting the challenge of modeling cloud and precipitation microphysics. *Journal of Advances in Modeling Earth Systems*, *12*(8). https://doi.org/10.1029/2019MS001689

Morrison, H., van Lier-Walqui, M., Kumjian, M. R., & Prat, O. P. (2020). A Bayesian approach for statistical–physical bulk parameterization of rain microphysics. Part I: Scheme description. *Journal of the Atmospheric Sciences*, *77*(3), 1019–1041. https://doi.org/10.1175/JAS-D-19-0070.1

Seifert, A., & Beheng, K. D. (2001). A double-moment parameterization for simulating autoconversion, accretion and selfcollection. *Atmospheric Research*, *59–60*, 265–281. https://doi.org/10.1016/S0169-8095(01)00126-0

Seifert, A., & Beheng, K. D. (2006a). A two-moment cloud microphysics parameterization for mixed-phase clouds. Part 1: Model description. *Meteorology and Atmospheric Physics*, *92*(1–2), 45–66. https://doi.org/10.1007/s00703-005-0112-4

Seifert, A., & Beheng, K. D. (2006b). A two-moment cloud microphysics parameterization for mixed-phase clouds. Part 2: Maritime vs. continental deep convective storms. *Meteorology and Atmospheric Physics*, *92*(1–2), 67–82. https://doi.org/10.1007/s00703-005-0113-3

Seifert, A., & Rasp, S. (2020). Potential and limitations of machine learning for modeling warm-rain cloud microphysical processes. *Journal of Advances in Modeling Earth Systems*, *12*(12). https://doi.org/10.1029/2020MS002301

Shima, S., Kusano, K., Kawano, A., Sugiyama, T., & Kawahara, S. (2009). The super-droplet method for the numerical simulation of clouds and precipitation: A particle-based and probabilistic microphysics model coupled with a non-hydrostatic model. *Quarterly Journal of the Royal Meteorological Society*, *135*(642), 1307–1320. https://doi.org/10.1002/qj.441

Shipway, B. J., & Hill, A. A. (2012). Diagnosis of systematic differences between multiple parametrizations of warm rain microphysics using a kinematic framework. *Quarterly Journal of the Royal Meteorological Society*, *138*(669), 2196–2211. https://doi.org/10.1002/qj.1913

Tzivion, S., Feingold, G., & Levin, Z. (1987). An efficient numerical solution to the stochastic collection equation. *Journal of the Atmospheric Sciences*, *44*, (21), 3139–3149. https://doi.org/10.1175/1520-0469(1987)044<3139:aenstt>2.0.co;2

Tzivion, S., Reisin, T. G., & Levin, Z. (1999). A numerical solution of the kinetic collection equation using high spectral grid resolution: A proposed reference. *Journal of Computational Physics*, *148*(2), 527–544. https://doi.org/10.1006/jcph.1998.6128

van Lier-Walqui, M., Morrison, H., Kumjian, M. R., Reimel, K. J., Prat, O. P., Lunderman, S., & Morzfeld, M. (2020). A Bayesian approach for statistical–physical bulk parameterization of rain microphysics. Part II: Idealized Markov chain Monte Carlo experiments. *Journal of the Atmospheric Sciences*, *77*(3), 1043–1064. https://doi.org/10.1175/JAS-D-19-0071.1

Wang, Y., Fan, J., Zhang, R., Leung, L. R., & Franklin, C. (2013). Improving bulk microphysics parameterizations in simulations of aerosol effects. *Journal of Geophysical Research: Atmospheres*, *118*(11), 5361–5379. https://doi.org/10.1002/jgrd.50432

Xue, L., Fan, J., Lebo, Z. J., Wu, W., Morrison, H., Grabowski, W. W., et al. (2017). Idealized simulations of a squall line from the MC3E field campaign applying three bin microphysics schemes: Dynamic and thermodynamic structure. *Monthly Weather Review*, *145*(12), 4789–4812. https://doi.org/10.1175/MWR-D-16-0385.1